Characterization of the Ensemble of Lignin-Remodeling DyP-Type Peroxidases from Streptomyces coelicolor A3(2)

Authors:

Hegne Pupart, Piia Jõul, Melissa Ingela Bramanis, Tiit Lukk

Date Submitted: 2023-02-22

Keywords: lignin remodeling, DyP-type peroxidases, Actinobacteria

Abstract:

Lignin is Nature's major source of aromatic chemistry and is by many seen as the green entry-point alternative to the fossil-based chemical industry. Due to its chemically recalcitrant structure, the utilization of lignin is challenging, wherein enzymes might be the key to overcome this challenge. Here, we focus on the characterization of dye-decolorizing peroxidases from Streptomyces coelicolor A3(2) (ScDyPs) in the context of enzymatic modification of organosolv lignins from aspen and Miscanthus × giganteus. In this study, we show that the ScDyPB can remodel organosolv lignins from grassy biomass, leading to higher molecular weight species, while ScDyPAs can deconstruct hardwood lignin, leading to an overall reduction in its molecular weight. Additionally, we show that ScDyPB is effective in polymerizing low-molecular-weight phenolics, leading to their removal from the solution.

Record Type: Published Article

Submitted To: LAPSE (Living Archive for Process Systems Engineering)

Citation (overall record, always the latest version):	LAPSE:2023.3837
Citation (this specific file, latest version):	LAPSE:2023.3837-1
Citation (this specific file, this version):	LAPSE:2023.3837-1v1

DOI of Published Version: https://doi.org/10.3390/en16031557

License: Creative Commons Attribution 4.0 International (CC BY 4.0)

energies

MDPI

Article

Characterization of the Ensemble of Lignin-Remodeling DyP-Type Peroxidases from *Streptomyces coelicolor* A3(2)

Hegne Pupart, Piia Jõul, Melissa Ingela Bramanis and Tiit Lukk *

Department of Chemistry and Biotechnology, Tallinn University of Technology, Akadeemia tee 15, 12618 Tallinn, Estonia

* Correspondence: tiit.lukk@taltech.ee

Abstract: Lignin is Nature's major source of aromatic chemistry and is by many seen as the green entry-point alternative to the fossil-based chemical industry. Due to its chemically recalcitrant structure, the utilization of lignin is challenging, wherein enzymes might be the key to overcome this challenge. Here, we focus on the characterization of dye-decolorizing peroxidases from *Streptomyces coelicolor* A3(2) (*Sc*DyPs) in the context of enzymatic modification of organosolv lignins from aspen and *Miscanthus* × *giganteus*. In this study, we show that the *Sc*DyPB can remodel organosolv lignins from grassy biomass, leading to higher molecular weight species, while *Sc*DyPAs can deconstruct hardwood lignin, leading to an overall reduction in its molecular weight. Additionally, we show that *Sc*DyPB is effective in polymerizing low-molecular-weight phenolics, leading to their removal from the solution.

Keywords: lignin remodeling; DyP-type peroxidases; Actinobacteria

check for updates

Citation: Pupart, H.; Jõul, P.; Bramanis, M.I.; Lukk, T. Characterization of the Ensemble of Lignin-Remodeling DyP-Type Peroxidases from *Streptomyces coelicolor* A3(2). *Energies* **2023**, *16*, 1557. https://doi.org/10.3390/en16031557

Academic Editor: Jeong-Hun Park

Received: 30 December 2022
Revised: 21 January 2023
Accepted: 25 January 2023
Published: 3 February 2023

Copyright: © 2023 by the authors. Licensee MDPI, Basel, Switzerland. This article is an open access article distributed under the terms and conditions of the Creative Commons Attribution (CC BY) license (https://creativecommons.org/licenses/by/4.0/).

1. Introduction

Lignocellulosic biomass (LCB) is Earth's most abundant renewable raw material [1]. This sustainable feedstock makes an attractive alternative to fossil-based resources to obtain bio-based materials, second-generation biofuels, bioenergy, value-added products, and chemicals [2–4]. LCB comprises three biopolymers: cellulose, hemicellulose, and lignin, with a typical ratio of 4:3:3, which varies among different species [5,6].

Lignin represents the second most abundant natural polymer after cellulose and constitutes the most abundant phenolic biopolymer on Earth [7]. Therefore, lignin is by many seen as a green entry-point alternative to fossil-based sources for the chemical industry [8,9]. The content of lignin varies significantly among hardwoods, softwoods, and herbaceous plants, wherein the highest content of lignin is in softwoods and the lowest in grasses [10].

Lignin is constructed from three monolignols—coniferyl alcohol, sinapyl alcohol, and *p*-coumaryl alcohol—which differ by the degree of methoxylation. When incorporated into lignin, those monolignols make up guaiacyl (G), syringyl (S), and hydroxyphenyl (H) units, respectively (Figure 1) [7,11]. The composition and type of lignin depend on the plant type. While softwood lignins primarily comprise guaiacyl units (G-type lignin), hardwood lignins also contain syringyl units (G/S-type lignin). Lignins in grassy biomass are built up from all three sub-units and, in addition to the previous two, contain substantial amounts of hydroxyphenyl units (G/S/H-type lignin) [10,12].

Since monolignol coupling involves radicals, there are many possibilities for linkages between lignin monomers. These sub-units are primarily connected by ether and carbon-carbon linkages, wherein β-aryl ether (β-O-4) linkages are the most common ones in softwood and hardwood lignins, approximately 50% and 60%, respectively (Figure 1). C-C linkages are less common in hardwood than in softwood lignins, as the additional methoxy groups, chiefly in the S units, hamper the formation of these linkages [12,13].

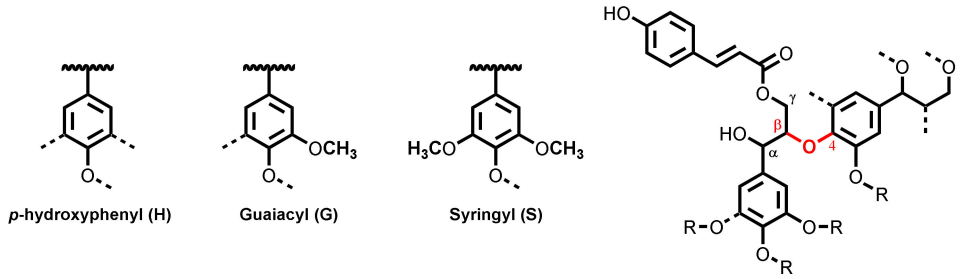

Figure 1. Lignin monomers with potential branchpoints marked with a dashed line; a structure of a possible lignin fragment containing the β-O-4 aryl ether linkage.

In addition to the source of lignin, the composition and molecular weight depend on the extraction method [12]. Most of the technical lignins are obtained by recovery as an industrial by-product [14]. The pulp and paper industries are the primary producers of technical lignin generating 50–70 million tons annually [15]. In contrast to the more traditional Kraft process, organosolv pulping utilizes organic solvents to dissolve lignin from the biomass [12]. It is an potent method for biorefineries for the utilization of biomass from hard- and softwoods as well as from grasses [12,16,17]. Organosolv lignin is highly pure, homogeneous, sulfur-free, with low content of carbohydrates and ash, and has a low molecular weight and dispersity. It is highly similar to native lignin, containing fewer modifications, and has an increased number of aryl ether linkages. So far, this technology has only reached pilot and demonstration scale, and not the industrial scale, mainly due to the high cost of solvent recovery [6,12,18].

Approximately only 2% of industrial lignin leftovers are used for commercial products [4,19]. Instead of being a mere by-product, lignin could be a useful co-product to produce valuable chemicals, such as vanillin [20]. Structurally extensively modified technical lignins with rearranged structures hinder its depolymerization into smaller fragments, a crucial and critical step for lignin utilization [21,22].

In nature, lignin decomposition is accomplished by numerous organisms, such as white-, brown-, and soft-rot fungi [23], and several Gram-positive and Gram-negative bacteria, mostly Actinobacteria and Proteobacteria [24]. In addition to other Streptomycetes, *Streptomyces coelicolor* has been identified as a lignin-degrading bacterial species, which harbors genes responsible for the catabolism of naturally occurring phenolics [25].

Lignin degraders, in nature, employ sophisticated metabolic and enzyme systems to attack and depolymerize lignin. Lignin-modifying enzymes, the key enzymes in lignin depolymerization, are phenol oxidases (laccases, EC 1.10.3.2) and heme-containing peroxidases—lignin-modifying peroxidases (LMPs): lignin peroxidase (LiP, EC 1.11.1.14), manganese(-dependent) peroxidase (MnP, EC 1.11.1.13), and versatile peroxidase (VP, EC 1.11.1.16). LMPs are part of the fungal class II heme-containing peroxidases in the catalase-peroxidase superfamily. These three ligninolytic peroxidases share noticeably high sequence identity and similarities in their structure [26,27].

Dye-decolorizing peroxidases (DyPs) also belong to LMPs but are phylogenetically unrelated to other LMPs (LiP, MnP, and VP). These peroxidases have heme as the attached prosthetic group and require hydrogen peroxide as the co-substrate that is reduced to water during its catalytic cycle [28]. DyPs (EC 1.11.1.19), systematically reactive-blue-5: hydrogen-peroxide oxidoreductases, were first identified in the fungus *Bjerkandera adusta* (previously *Geotrichum candidum* 1 Dec) in 1999 [29], later in bacteria [26]. Because of their distinctive structural and catalytic characteristics, DyPs form a new group of heme peroxidases [30]. They were named based on their ability to degrade and decolorize anthraquinone and azo dyes, such as Reactive Blue 5 [29,31,32]. The substrate specificity of DyPs is broad; in addition to dyes, they also oxidize other typical peroxidase substrates such as 2,2′-azino-bis(3-ethylbenzothiazoline-6-sulfonic acid (ABTS) and 2,6-dimethoxyphenol (2,6-DMP) [26,33]. DyPs can oxidize phenolic [34] and non-phenolic lignin fragments without requiring a mediator [35,36].

According to the phylogenetic analysis of genomic sequences, DyPs have been classified into four sub-families in PeroxiBase. Sub-families A, B, and C contain predominately bacterial peroxidases, while sub-family D peroxidases are from fungi [37]. A newer classification was proposed in 2015, which divides DyPs into classes P (primitive, former class B), I (intermediate, former class A), and V (advanced, former classes C and D) [38]. DyP-type peroxidases are more or less considered bacterial counterparts to fungal LMPs [39]. The ability to decompose lignin has been identified from several DyPs. It includes peroxidases from fungi *Auricularia auricula-judae* [35], *Irpex lacteus* [40], and bacterial species such as *Rhodococcus jostii* [41], *Thermobifida fusca* [42], and *Pseudomonas fluorescens* [43]. *S. coelicolor* A3(2) genome was sequenced in 2002 [44] and has three genes encoding DyPs, two A-type DyPs and a B-type DyP. We hypothesize that this bacterium requires dye-decolorizing peroxidases to metabolize lignin.

Here, we cloned, expressed, and purified all three DyPs encoded by *S. coelicolor* A3(2). The H_2O_2-dependent activity of the enzymes were characterized using a soluble model substrate ABTS as well as water-insoluble organosolv lignins from *Miscanthus* × *giganteus* and aspen. The activity of DyPs on ABTS did not correlate with their ability in modifying lignin, a phenomenon that may reflect different pH optima observed with these two substrates. Furthermore, different DyPs had distinctly different effects in lignin modification. Treatment of lignins with type-A DyPs, *Sc*DyP1A and *Sc*DyP2A, resulted in depolymerization of lignin, whereas treatment with *Sc*DyPB increased the molecular weight of lignin.

2. Materials and Methods

In order to conserve space, portions containing detailed information about the experiments can be found in the Supplementary Materials.

2.1. Gene Cloning

Genes encoding dye-decolorizing peroxidases (DyPs) (accession numbers: NP_626524.1, NP_628147.1, and NP_631251.1 for locus tags SCO2276 (*Sc*DyP1A), SCO3963 (*Sc*DyP2A), and SCO7193 (*Sc*DyPB), respectively) were amplified from *Streptomyces coelicolor* A3(2) genomic DNA using the oligonucleotide primers with restriction endonuclease sites for NdeI and XhoI, respectively (Table S1). Plasmid DNAs were purified by alkaline lysis. The amplified genes (1263 bp, 1338 bp, and 951 bp for SCO2276, SCO3963, and SCO7193, respectively) were cloned into pET15b expression vector coding for an N-terminal His_6-tag followed by thrombin protease site. Additionally, codon-optimized genes for SCO2276 and SCO3963 were obtained and pre-cloned into the pET28a expression vector (Twist Bioscience, San Francisco, CA, USA). Each clone (codon-optimized) carried the Kan resistance gene, N-terminal His_6-tag, and thrombin cleavage site.

2.2. Overexpression

Recombinant *Sc*DyPs were overproduced in *E. coli* BL21 (DE3) as His_6-fusion proteins (without the N-terminal 40-amino acid putative twin-arginine translocation (Tat) signal peptides in the case of *Sc*DyPAs). The overnight starter cultures were used for inoculation. The culture media (LB prepared in tap water) supplemented with antibiotics was incubated at 37 °C until the OD_{600} reached 0.6–0.8. The overexpression of recombinant protein was induced by 1 mM isopropyl-β-D-1-thiogalactopyranoside. The culture was grown overnight, at 30 °C and 180 rpm. The cells were harvested at 4000 g, 15 min, and 4 °C.

2.3. Purification

The harvested cells were resuspended in buffer A (20 mM Tris-HCl, pH 7.5, 0.5 M NaCl, 5 mM imidazole) and lysed using sonication (Bandelin Sonopuls, Bandelin GmbH & Co, Berlin, Germany) or high-pressure homogenization (EmulsifFex-C5, Avestin, Ottawa, ON, Canada). The lysed cells were centrifuged at 35,000 g for 1 h, at 4 °C. The supernatant was loaded onto the HisTrap FF column (GE Healthcare, Chicago, IL, USA). The column was washed with 10 column volumes (CV) of 10% buffer B (20 mM Tris-HCl, pH 7.5, 0.5 M NaCl,

0.5 M imidazole) to remove non-specifically bound proteins. The His_6-tagged protein was eluted with the linear gradient of imidazole of 10 to 100% buffer B (20 CV). The fractions were analyzed with SDS-PAGE, and the protein of interest was pooled. His_6-tag was cleaved by overnight incubation with thrombin (2 U per 1 mg protein) at 4 °C. The heme reconstitution was conducted with hemin (2-fold molar excess) at room temperature for 2 h using 20 mg/mL hemin (98%, porcine, Acros Organics, Fair Lawn, NJ, USA) dissolved in DMSO. The protein was exchanged to 20 mM Tris-HCl buffer (pH 7.5) containing 0.1 M NaCl (HiPrep 26/10 Desalting column) (GE Healthcare); the resulting protein fractions were pooled and concentrated using centrifugal filters with a molecular weight cutoff of 10 kDa (Sartorius, Göttingen, Germany). The protein was flash-frozen in liquid nitrogen and stored at −80 °C.

2.4. Determination of Enzyme Concentration

The total protein concentration was determined spectrophotometrically at 280 nm (UV-2700 UV-Visible Spectrophotometer, Shimadzu, Japan). The extinction coefficient ε280 nm values, calculated using the Expasy ProtParam tool (https://web.expasy.org/protparam/, accessed on 15 August 2022), were 51,450; 38,960; and 18,450 $M^{-1}cm^{-1}$, for *Sc*DyP1A, *Sc*DyP2A, and *Sc*DyPB, respectively. To estimate the total protein concentration before heme reconstitution, the buffer was exchanged using ultrafiltration filters to prevent concentration overestimation due to imidazole absorption.

The amount of active enzyme (with heme in the active site) was calculated using characteristic absorbance at 406 nm (ε_{406} = 100,000 M^{-1} cm^{-1}) for heme proteins [45]. The total and the active enzyme content was calculated before and after the reconstitution with hemin. The heme content of DyPs was evaluated by Reinheitszahl value (Rz, A_{406}/A_{280}). In all experiments, the enzymes were dosed based on the active enzyme concentration.

2.5. Enzyme Assays

All enzyme assays with ABTS (ChemCruz™, Santa Cruz, CA, USA) were performed in triplicate using Shimadzu UV-2700 UV-Visible Spectrophotometer at room temperature (except for the investigation of temperature dependence). All measurements with 100 nM *Sc*DyP1A, 50 nM *Sc*DyP2A, or 15 nM *Sc*DyPB were used. Oxidation of ABTS was carried out with 1 mM H_2O_2, and the formation of ABTS cation radical was measured at 420 nm (ε_{420} = 36,000 M^{-1} cm^{-1}). A fresh stock solution of H_2O_2 was prepared daily before use. The stock of 2,6-DMP (Acros Organics, Fair Lawn, NJ, USA) was prepared in dimethylformamide. The oxidation of 2,6-DMP was measured at 470 nm (ε_{470} = 53,200 M^{-1} cm^{-1}) [46]. Optimal pH and temperature dependence parameters were determined (Supplementary Materials). The data analysis was carried out using OriginPro 2021 software (OriginLab, Northampton, MA, USA).

2.6. Organosolv Extraction of Lignin

Ethanol organosolv lignin from bleached chemi-thermomechanical aspen pulp was extracted as described in Jõul et al., 2022 [16]. Ethanol organosolv lignin from *Miscanthus* × *giganteus* (*Mxg*-lignin) was provided by Stefan Bauer [17]. Klason analysis was conducted as described in Jõul et al., 2022 [16] to determine the total lignin content for aspen (86.8 ± 0.7%) and *Mxg* (85.0 ± 1.1%) lignins, respectively.

2.7. Enzymatic Treatment of Organosolv Lignins

Ethanol organosolv lignin suspension at 1 mg/mL in aqueous HEPES (Sigma-Aldrich, St. Louis, MO, USA), buffer (50 mM, pH 8.0) with added 2 mM H_2O_2 was treated with 10 µM of *Sc*DyP1A, *Sc*DyP2A, or *Sc*DyPB, incubated for 24 h, at 28 °C. For turbidity, the reaction mixtures were agitated at 200 rpm. The reaction mixtures and controls were centrifuged, and the insoluble portions were lyophilized for storage. The supernatants were extracted with ethyl acetate for further analysis. The water-insoluble portions of lignin

were analyzed via gel permeation chromatography (GPC) and water-soluble portions with gas chromatography-mass spectrometry (GC-MS).

3. Results

3.1. The Ensemble of DyP-Peroxidases of Streptomyces coelicolor

The genome of *S. coelicolor* A3(2) (*Sc*) carries three genes encoding for DyPs: two type-A DyPs, *Sc*DyP1A (SCO2276) and *Sc*DyP2A (SCO3963), and a type-B DyP, *Sc*DyPB (SCO7193) with molecular weights of 45 kDa, 47 kDa, and 34 kDa, respectively. The three genes are located in three distinct loci on the single linear chromosome of *S. coelicolor.* Regarding the operonic context, it is not entirely clear what specific biological role *Sc*DyPB might be involved with. However, in the case of *Sc*DyP1A, the annotations of the neighboring genes in its operon suggest its role in iron homeostasis (i.e., iron permease, high-affinity iron-transporter, etc.). In contrast, in the case of *Sc*DyP2A, the operon contains a putative prephenate dehydrogenase and an aminoacyl-tRNA synthetase, thus suggesting a role in the biosynthesis of aromatic amino acids, which is well aligned with lignin biochemistry (Table 1). The genes of *Sc*DyP1A and *Sc*DyP2A contain an N-terminal Tat secretion tag, suggesting a role outside of the cytosole, whereas *Sc*DyPB lacks the secretion signal, suggesting a biochemical role inside the cell.

Table 1. The annotations of DyP-type peroxidases of *S. coelicolor* A3(2) and their corresponding operon neighbors, as assigned in the public databases.

***Sc*DyP**	**Locus Tag**	**Annotation [1]**
***Sc*DyPB**	**SCO7193**	**putative iron-dependent peroxidase**
	SCO7192	sigma factor
	SCO7194	putative polysaccharide biosynthesis protein
***Sc*DyP1A**	**SCO2276**	**ferrous iron transport peroxidase**
	SCO2272, SCO2274	heme ABC transporter
	SCO2273	hemin transport system permease
	SCO2275	ferrous iron transport periplasmic protein
	SCO2277	ferrous iron transport permease
	SCO2278	hypothetical protein
***Sc*DyP2A [2]**	**SCO3963**	**DyP-type peroxidase family protein**
	SCO3971	conserved hypothetical protein
	SCO3970	Xaa-Pro aminopeptidase
	SCO3969	possible ATP/GTP-binding protein
	SCO3968	putative integral membrane protein
	SCO3967	putative membrane protein
	SCO3966, SCO3965	putative copper metallochaperone
	SCO3964	copper transport protein
	SCO3962	prephenate dehydratase
	SCO3961	seryl-tRNA synthetase
	SCO3960	hydrolase (HAD superfamily)

[1] Annotation is based on JGI IMG/M and the SEED databases. [2] The operon for *Sc*DyP2A is encoded on the complement strand.

3.2. Production and Purification of Recombinant ScDyPs

*Sc*DyPs were expressed as His-tagged fusion proteins in *E. coli*, purified, and the concentration of apo- and holo-enzymes determined using spectrophotometry. The *Sc*DyPs showed the typical heme-peroxidase spectrum with a Soret band maxima at 408 nm, 405 nm and 401 nm for *Sc*DyP1A, *Sc*DyP2A, and *Sc*DyPB, respectively (Figure S1). The heme content of peroxidases was evaluated by Rz value (Table 2). Before reconstitution with hemin, the highest heme content was observed with *Sc*DyPB followed by *Sc*DyP1A and *Sc*DyP2A (Table 2). The reconstitution improved the proportion of holo-enzyme (Table 2)—1.7-fold for *Sc*DyP1A and 2.2-fold for *Sc*DyP2A—while for *Sc*DyPB, the Rz ratio remained relatively the same. In order to tackle the low expression yields of *Sc*DyPAs (about 1 mg of protein from 1 L culture) from plasmids containing inserts of PCR-amplified genomic DNA

(i.e., 1 mg of protein for *Sc*DyP1A/*Sc*DyP2A from 1 L culture), synthetic genes that were codon-optimized for expression from an *E. coli* host, were obtained. The proteins were then expressed and purified, where *Sc*DyP1A had an Rz value of 2.01 and *Sc*DyP2A 2.02 before reconstitution with hemin. The reconstitution of DyPAs from the codon-optimized system with hemin did not show a particular effect, as the Rz values remained the same. The codon-optimization of genes considerably improved the protein expression yield for both *Sc*DyP1A and *Sc*DyP2A.

Table 2. Reinheitszahl values of *Sc*DyPs before and after the heme reconstitution.

Rz Value	*Sc*DyP1A	*Sc*DyP2A	*Sc*DyPB	*Sc*DyP1A [CO]	*Sc*DyP2A [CO]
Before reconstitution with hemin	0.78 ± 0.02	0.51 ± 0.02	2.36 ± 0.04	2.01 ± 0.11	2.02 ± 0.01
After reconstitution with hemin	1.33 ± 0.08	1.14 ± 0.02	2.32 ± 0.07	1.92 ± 0.03	2.17 ± 0.03

[CO] Codon optimized genes for the expression out of *E. coli* BL21 (DE3).

3.3. Biochemical Characterization

3.3.1. Optimal pH for *Sc*DyPs

The pH dependency of the oxidation of ABTS is shown in Figure 2. *Sc*DyP1A and *Sc*DyP2A exhibited the highest activity at pH 3.5, while the optimal pH for *Sc*DyPB was determined to be 3.0 (Figure 2). At pH 5.0, all *Sc*DyPs showed almost no activity with ABTS. Contrary to ABTS, the oxidation of phenolic substrate (2,6-DMP) by *Sc*DyP2A and *Sc*DyPB had a pH optimum around 8.5 (data not shown). *Sc*DyP1A did not catalyze the oxidation of 2,6-DMP.

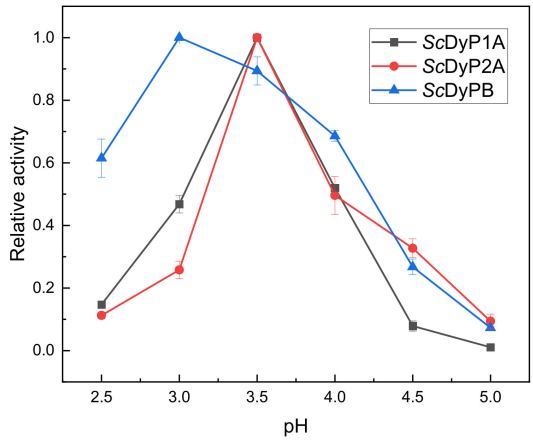

Figure 2. Optimum pH of dye-decolorizing peroxidases of *S. coelicolor* toward oxidation of ABTS. Data are average values of three independent measurements.

3.3.2. Temperature Dependency

The temperature dependency on enzyme activity was measured at pH 3.5 using ABTS as the substrate. Peroxidase activity for all DyPs were at a decline or started decreasing already at 30 °C and decreased with further temperature increase (Figure 3).

3.3.3. Thermostability

To further estimate the temperature stability of *Sc*DyPs, the enzyme solutions were incubated, at 30 °C, for 48 h, and at fixed time intervals, sample aliquots were withdrawn, and tested for activity. Within 2 h, *Sc*DyP2A had lost most activity compared to other *Sc*DyPs, approximately one-third (Figure 4). After 24 h, *Sc*DyP1A and *Sc*DyPB had lost ~20% of activity, and *Sc*DyP2A had around half of its activity. *Sc*DyP1A is the most thermoresistant *Sc*DyP and had retained ~70% of its activity within 48 h, wherein *Sc*DyP2A had lost ~70% of its activity.

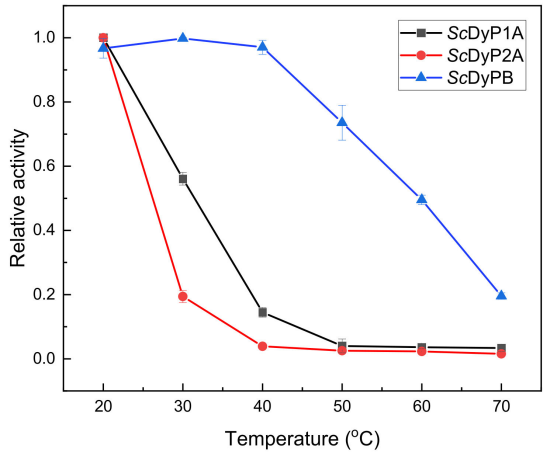

Figure 3. The temperature dependency of *Sc*DyPs. Peroxidase activity was measured at pH 3.5 (50 mM sodium citrate) using ABTS as substrate. 1 mM H_2O_2 was used as a co-substrate. Experiments were conducted in triplicate.

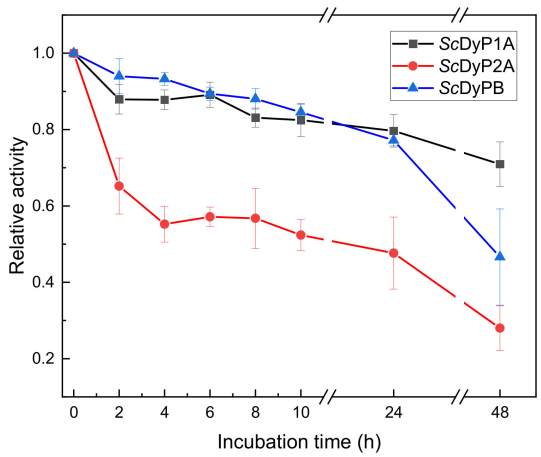

Figure 4. Thermostability of *Sc*DyPs. The enzyme stocks were incubated in 50 mM sodium citrate (pH 3.5), at 30 °C. At selected times, the activities were measured using ABTS and 1 mM H_2O_2. Experiments were conducted in triplicate.

3.3.4. Steady-State Kinetics

Steady-state kinetic measurements were conducted at pH 3.5, varying the concentration of ABTS and using 1 mM H_2O_2 as a co-substrate. All *Sc*DyPs displayed non-Michaelis-Menten kinetics (Figure S2), and the results were analyzed using the equation accounting for substrate inhibition (Equation (S1) in the Supplementary Materials). Kinetic parameters are summarized in Table 3. Highest k_{cat} was measured with *Sc*DyPB, followed by *Sc*DyP2A and *Sc*DyP1A. The *Sc*DyPB had also the lowest apparent K_M values for ABTS. Owing to its high k_{cat} and low K_M value, the *Sc*DyPB had by far the highest catalytic efficiency (k_{cat}/K_M) in oxidation of ABTS (Table 3). All three DyPs are inhibited by increased substrate concentrations, wherein *Sc*DyPB is more prone to inhibition by ABTS with a K_i of 0.4 mM (Table 3; Figure S2). 2,6-DMP was also tested as a substrate but proved to be a poor substrate for *Sc*DyPs, especially for *Sc*DyP1A, which did not oxidize this substrate (data not shown). However, the apparent specificities (k_{cat}/K_M) were approximately 140-fold lower for *Sc*DyP2A (~0.1 $mM^{-1}\cdot s^{-1}$) and approximately 200-fold lower for *Sc*DyPB (~3.1 $mM^{-1}\cdot s^{-1}$). Similarly, substrate inhibition was seen with 2,6-DMP (Figure S3).

Table 3. Kinetic parameters for the oxidation of soluble model substrate ABTS by *Sc*DyPs. Apparent steady-state kinetic parameters were measured at pH 3.5 using 1 mM H_2O_2 as a co-substrate. Data are average values of three independent measurements.

	***Sc*DyP1A**	***Sc*DyP2A**	***Sc*DyPB**
K_M (mM)	1.4 ± 0.15	2.3 ± 0.9	0.08 ± 0.02
k_{cat} (s^{-1})	7.6 ± 1.1	31.7 ± 14.6	48.6 ± 5.7
k_{cat}/K_M ($mM^{-1} \cdot s^{-1}$)	5.4 ± 0.2	13.8 ± 1.3	607 ± 95.2
K_i (mM)	4.3 ± 1.4	1.6 ± 1.0	0.4 ± 0.1

3.4. Lignin Remodeling Activity of ScDyPs

3.4.1. Identification of Molecular Weight Distribution of Lignin Samples by GPC Analysis

GPC analysis was utilized to observe the changes in the relative size distribution of *Sc*DyPs-treated organosolv *Mxg*- and aspen lignins. Lignins were incubated in the presence of *Sc*DyPs for 24 h, then centrifuged, and the pellets were lyophilized. For the GPC analysis, the lyophilized pellets were dissolved in THF, and the molecular weights of lignins were observed. The number-average molecular weight (Mn) of *Mxg*-lignin was 1509 Da, and the weight-average molecular weight (Mw) 2435 Da (Table 4).

Table 4. Mn, Mw, and the molar-mass dispersity ($Đ_M$) of *Mxg*- (panel A) and aspen (panel B) ethanol organosolv lignins treated with *Sc*DyPs determined by GPC analysis. Solutions containing lignins at 1 mg/mL in HEPES buffer (pH 8.0) and 2 mM H_2O_2 without enzymatic treatment, or treated with 10 μM enzyme were incubated for 24 h. Samples were centrifuged, pellets lyophilized and dissolved, and the lignins were analyzed using GPC.

	***Mxg*-Lignin**			**Aspen Lignin**		
	Mn	**Mw**	**$Đ_M$**	**Mn**	**Mw**	**$Đ_M$**
Without enzyme	1509 ± 10	2435 ± 35	1.61	2772 ± 51	5533 ± 53	2.0
+*Sc*DyP1A	1502 ± 8	2357 ± 26	1.57	2589 ± 12	4705 ± 72	1.82
+*Sc*DyP2A	1489 ± 11	2332 ± 45	1.57	2429 ± 106	4371 ± 258	1.8
+*Sc*DyPB	1856 ± 21	2921 ± 28	1.57	2994 ± 33	5607 ± 79	1.87

At first, pH 3.5 was used for the lignin experiments, but the lignin treatment at acidic media did not show an effect. Acidic to alkaline pH ranges were tested for optimal lignin-remodeling activity, where a pH range of 7.5 to 8.5 was deemed the most active (data not shown). The treatment of *Mxg*-lignin with *Sc*DyPB led to the polymerization of lignin polymer up to 19%. Similar behavior was seen with aspen lignin. The enzymatic treatment with *Sc*DyPB caused the increase in lignin molecular weight, whereas *Sc*DyPAs showed the ability to decrease the molecular weight of lignin. The Mn of *Mxg* organosolv lignin treated with *Sc*DyP2A and with *Sc*DyP1A remained the same as with untreated material. However, the Mw of aspen lignin after 24 h treatment with *Sc*DyP2A decreased by approximately 20%. Similarly, a reduction in the average molecular weight of aspen lignin after *Sc*DyP1A treatment could also be detected. The $Đ_M$ of *Mxg*-lignin fragments decreased from 1.61 to 1.57. The $Đ_M$ of aspen lignin decreased from 2.00 to 1.87 (*Sc*DyPB), 1.80 (*Sc*DyP2A), and 1.82 (*Sc*DyP1A). According to these results, all three *Sc*DyPs can remodel organosolv lignin, wherein the *Mxg*-lignin is a better substrate for *Sc*DyPB and aspen lignin for *Sc*DyPAs (Figure 5).

3.4.2. Identification of Low-Molecular-Weight Compounds in Lignin Samples by GC-MS Analysis

GC-MS analysis was used to determine the low-molecular-weight (LMW) compounds in lignin samples. The organosolv lignins were incubated with and without *Sc*DyPs for 24 h and centrifuged; the supernatants were extracted with ethyl acetate, lyophilized, dissolved in methanol, and analyzed with GC-MS. According to the GC-MS results, the

LMW proportion of *Mxg*-lignin contains mostly H-units, fewer G-units, and a small portion of S-units, wherein aspen lignin is in the most part composed of S-units, fewer G-units, and a minute proportion of H-units (based on the integrated peak area). The treatment of both lignins with *Sc*DyPs decreased the amount of LMW compounds found in supernatants, where *Sc*DyPB had the highest effect (Table 5).

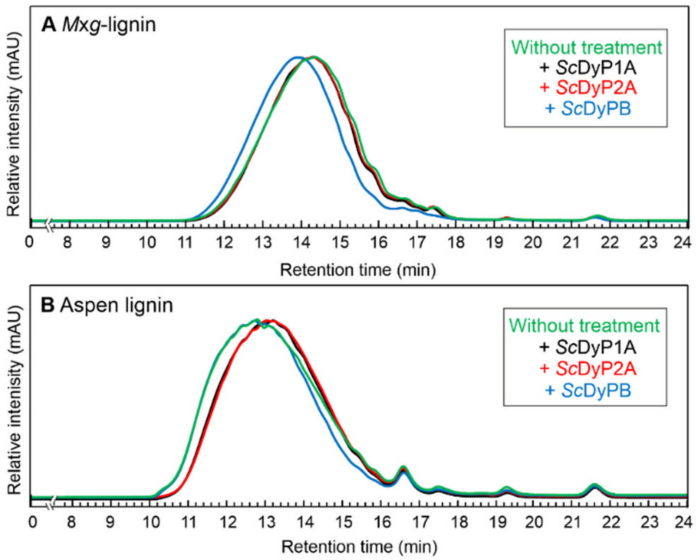

Figure 5. The characterization of lignin-remodeling activities of *Sc*DyPs by GPC. Panel (**A**) *Mxg*-lignin, panel (**B**) aspen lignin. The treatment of *Mxg*-lignin with *Sc*DyPB led to the polymerization of lignin polymer. The treatment of aspen lignin with *Sc*DyPAs resulted in lignin depolymerization.

Table 5. The most prominent LMW compounds found in *Mxg*-lignin (A) and aspen lignin (B), and the influence of *Sc*DyPs treatment to the peak area reduction. The peak areas are represented in percentages where the result from the untreated sample is set to 100%, and the treated samples are defined as the percentage peak area left after the treatment.

(A) Unit	Compound Name	Without Treatment	*Sc*DyP1A	*Sc*DyP2A	*Sc*DyPB
H	*p*-Hydroxycinnamic acid, ethyl ester	100	78	78	2
G	Ethyl (E)-ferulate	100	67	75	2
G	(E)-4-(3-Hydroxyprop-1-en-1-yl)-2-methoxyphenol	100	77	69	9
G	Glyceryl ferulate	100	87	95	nd *
S	*trans*-Sinapyl alcohol	100	63	69	5
(B) Unit	**Compound Name**	**Without Treatment**	**ScDyP1A**	**ScDyP2A**	**ScDyPB**
S	*trans*-Sinapyl alcohol	100	53	55	37
G	(E)-4-(3-Hydroxyprop-1-en-1-yl)-2-methoxyphenol	100	44	52	16
S	*trans*-Sinapaldehyde	100	64	68	53
G	Butyrovanillone	100	92	73	nd *
G	2-Propanone, 1-hydroxy-3-(4-hydroxy-3-methoxyphenyl)-	100	nd *	nd *	nd *

* not detected.

4. Discussion

The purpose of this study was to characterize the full ensemble of DyP peroxidases from *S. coelicolor* A3(2), which consists of two A-type and one B-type DyP peroxidase in the context of enzymatic modification of organosolv lignins. The physiological roles

of DyPs are unclear to date. It has been shown previously that some type-A DyPs are components of tripartite ferrous iron transporters and serve a role in iron uptake [47,48]. There are reports of DyPs functioning as deferrochelatases by releasing heme iron without tetrapyrrole degradation, such as EfeB (class A) from *E. coli* [49]. According to the operonic context, *Sc*DyP1A might be a ferrous iron transport peroxidase. B-type DyPs are putative cytoplasmic enzymes indicating a function in intracellular metabolism [50]. However, the operonic context of *Sc*DyPB does not hint at its specific role for *S. coelicolor*.

For the biochemical characterization, the three DyPs from *S. coelicolor* A3(2) were heterologously expressed and purified. The efficiency of heterologous expression of proteins is often hampered by differences in the codon usage between the organism of origin and the chosen host expression organism for a particular gene. In addition to differences in the abundance of specific tRNAs, the genome of *S. coelicolor* has 72% G + C content, when compared to that of about 51% of *E. coli*. [44,51]. Although the expression of *Sc*DyPB yielded sufficient amounts of enzyme for further experiments (20 mg per liter culture), the expression of *Sc*DyPAs resulted in roughly 20-fold less protein. Successful protein expression in *E. coli* as the host depends on several factors, such as the choice of the expression plasmid and the strain, the optimization of expression conditions, etc. [52,53]. However, codon usage seems to have the highest impact on obtaining high protein yields from recombinant expression [54]. It is also known that *S. coelicolor* has remarkably different codon usage profile than *E. coli* [55]. Codon optimization is often used to enhance the translation efficiency of a gene of interest [56]. It has been seen that codon-optimization results in an even 140-fold improvement of protein expression yield [57]. Here, the expression with codon-optimized genes enabled the production of higher quantities of protein when compared to the non-optimized construct, resulting in a 4-fold and 43-fold increase for *Sc*DyP1A and *Sc*DyP2A, respectively. Additionally, DyPs require heme as a prosthetic group for its catalytic activity [29]. Recombinant bacterial expression frequently produces heme-deficient proteins [58–61], which can be combated by supplementing the growth media with extra hemin during the expression [61]. Unfortunately, the heme transport systems of most *E. coli* strains cannot efficiently uptake hemin and depend on the diffusion through the cell membrane [60,61]. The Reinheitszahl (Rz) value (from German "purity number"), the ratio of absorbances (A_{Soret}/A_{280}), is used to obtain an estimate on the extent of heme incorporation into peroxidases. Prior to supplying the DyPs with additional hemin, Rz values of *Sc*DyP1A and *Sc*DyP2A were below one. The reconstitution improved the Rz values by approximately 2-fold for both *Sc*DyPAs. The Rz values for *Sc*DyPAs obtained from codon-optimized genes and *Sc*DyPB were over two without any extra steps. The heme reconstitution after purification did not increase the Rz values of *Sc*DyPAs obtained from codon-optimized genes and for *Sc*DyPB. It is fathomable that the uptake kinetics of heme by DyPAs in vivo are affected by the differences in the speed of translation between the high G + C non-optimized vs. codon-optimized DyPA constructs. Although we have no direct evidence for it, it is possible that there may be minor differences in protein folding due to ribosome stalling which may also affect the heme uptake by the purified proteins in vitro.

Having obtained sufficient amounts of heme-reconstituted *Sc*DyPs, we set out to determine their optimal working conditions (i.e., pH and temperature). DyP-type peroxidases have demonstrated a lower pH preference than classic heme peroxidases [29,62]. Typically, rather similar pH optima for ABTS and 2,6-DMP oxidation have been identified for DyPs. Previous studies of fungal and bacterial DyPs have reported that the optimum pH for ABTS and 2,6-DMP oxidation falls in the pH range of 3–5 [63–65]. Our results of *Sc*DyPs were consistent with the past findings for ABTS. The optimum pH of *Sc*DyPs for ABTS oxidation was determined in the range of 3–3.5, but in contrast, for phenolic 2,6-DMP oxidation, the optimum pH was 8.5. Chaplin et al., 2017 reported that the optimum pH for 2,6-DMP oxidation is 9.0 for DyPA from *Streptomyces lividans* [66]. This kind of phenomenon has also been seen in the case of laccases, where the enzymes catalyze the oxidation of ABTS better at pH 4, but the oxidation of 2,6-DMP at alkaline pH (7–9) [67,68].

It has been shown that enzymes isolated from extremophiles can tolerate more severe conditions, such as extremes in pH, temperature, salt concentration, etc., often required for industrial processes. For instance, the optimal temperature of A-type *Tc*DyP from a thermophilic actinomycete *Thermomonospora curvata* was also 30 °C; however, 1 h incubation of *Tc*DyP at 60 °C resulted in ~70% retained activity [69]. Since *S. coelicolor* is a mesophilic bacterium, it was expected that *Sc*DyPs would show only modest resistance to elevated temperatures. *Sc*DyPB showed the highest activity at 30 °C, and the activity of all *Sc*DyPs decreased with the rising temperature. The activities of *Sc*DyPAs decreased more rapidly at higher temperatures compared to *Sc*DyPB. The relative activity of *Sc*DyPB at 40 °C was 90%, but in contrast, *Sc*DyPAs had retained only less than 20% of activity. Further, the stability of *Sc*DyPs at 30 °C was determined (Figure 4). The thermostability of *Sc*DyP2A was decreasing most rapidly and, within 48 h, had lost 70% of its activity. *Sc*DyP1A was relatively stable for 48 h with residual activity of 70%. Min et al., 2015, had a novel observation where the optimum temperature of *Bs*DyP was dependent on the substrates the residual activity was measured with [36]. Therefore, temperature dependency and thermostability results were only compared to those where ABTS was used for the measurements.

All three DyPs possessed different apparent specificities (k_{cat}/K_M) for ABTS, 5 $mM^{-1}\cdot s^{-1}$, 14 $mM^{-1}\cdot s^{-1}$, and 600 $mM^{-1}\cdot s^{-1}$ for *Sc*DyP1A, *Sc*DyP2A, and *Sc*DyPB, respectively. Like *Sc*DyPs, the peroxidase activities are not comparable to C- and D-type DyPs and show much lower activities. Previously characterized DypA and DypB from *Rhodococcus jostii* RHA1, a Gram-positive soil bacteria, showed lower apparent specificities with ABTS than *Sc*DyPs, approximately 2 $mM^{-1}\cdot s^{-1}$ [41]. Substrate inhibition is a frequent phenomenon and occurs in roughly 25% of known enzymes [70]. Substrate inhibition was observed in case of all *Sc*DyPs, with both substrates, wherein with ABTS, *Sc*DyPA1 was inhibited the most and *Sc*DyPB the least.

According to in silico analysis by Benslama et al., 2022, it was proposed that a DyP from *S. coelicolor* (*Sc*DyP1A) has the potential to efficiently biodegrade lignin [71]. Lignin remodeling experiments with *Sc*DyPs were conducted with organosolv lignins from aspen and *Miscanthus* × *giganthus.* The acidic conditions (pH 3.5) initially used in lignin remodeling experiments were unsuitable, most probably due to the aggregation of DyPs at lower pH. Additionally, alkaline pH was preferred due to the substantially increased solubility of lignin in alkaline media (deprotonation of phenolic OH-groups) [9]. A range of alkaline pHs was tested, and pH 8 was chosen as the most promising pH for lignin experiments.

GPC analysis determined that the enzymatic treatment of lignin decreased the dispersity—$Đ_M$ [72] for both lignins—indicating that lignin becomes more homogeneous due to treatment with *Sc*DyPs. Neither of the A-type *Sc*DyPs had an effect on the molecular weight distribution of *Mxg*-lignin, while *Sc*DyPB did not affect the molecular weight distribution of aspen lignin. *Sc*DyP2A had the highest effect on lignin, and Mw of aspen lignin was reduced by ~20%. Treating *Mxg*-lignin with *Sc*DyPB led to lignin polymerization and led to the increase in the molecular weight of *Mxg*-lignin. This is a common problem, which is brought about by several condensation and polymerization routes, such as radical coupling, vinyl condensation, generation of reactive fragments involving polymerization, and reactive functional group-induced repolymerization reactions [73]. It has been observed that the success of lignin depolymerization is highly dependent on the nature of the lignin sample. In addition to the radical species generated, the ratio of phenolic/aliphatic OH-groups in lignin determines the fate of lignin [74]. A possible strategy to combat polymerization is to combine different enzymes. For instance, Rahmanpour et al., 2017, have identified an extracellular bacterial flavoenzyme that can prevent the repolymerization of lignin [75].

GC-MS analysis was used to analyze the supernatant of enzymatically treated or untreated lignins. Although this analysis does not determine the entire monolignol content of these lignin preparations, it was used to verify the main LMW compounds solely in the supernatant. According to GC-MS, the predominant LMW peak in *Mxg*-lignin belongs to an H-unit (p-Hydroxycinnamic acid ethyl ester), while in aspen lignin, the spectra is

dominated mostly by S-units. Several monolignols in *Mxg*-lignin were α-ethoxylated, a distinctive feature of ethanol organosolv lignins [17]. The results from GC-MS analysis provide one possible explanation for the results obtained from GPC analysis—the tendency of aspen lignin to be depolymerized and *Mxg*-lignin to be (re)polymerized. As S-units have a higher degree of methoxylation, the steric hindrance decreases the probability of crosslinking, and therefore, the depolymerization of lignin is promoted compared to polymerization. It has been reported previously that DyPs can be applied to coupling phenolic monomers [76]. Here, we similarly observed that after the enzymatic treatment, the number of monolignols in the supernatant decreased drastically. This observation might be explained by (i) the loss of lignin solubility caused by the enzymatic treatment and (ii) the polymerization of LMW compounds of lignins remaining in the pellet fraction after centrifugation.

5. Conclusions

Streptomyces coelicolor A3(2) is a rich source of enzymes with high potential for a variety of biotechnological applications. In addition to an extensively studied small laccase, the genome of *S. coelicolor* also encodes for several lytic polysaccharide monooxygenases and glycosyl hydrolases, but also an ensemble of dye-decolorizing peroxidases—*Sc*DyPs. Here, *Sc*DyPs were characterized in the context of their possible biotechnological application as lignin modifying enzymes. Using ABTS as the model substrate, pH and temperature dependence as well as Michaelis–Menten kinetic parameters were determined. *Sc*DyPB showed the highest rate of catalysis with ABTS compared to other *Sc*DyPs. Lignin remodeling activity was demonstrated with *Sc*DyPB, which polymerized grassy biomass derived organosolv lignin, and with *Sc*DyPAs, which depolymerized hardwood derived organosolv lignin. In addition to that, we demonstrated that *Sc*DyPB is an effective tool for the removal of water-soluble LMW phenolics.

Our results illustrate the relevance of ligninolytic enzyme characterization alongside characterization of lignin to understand and improve the enzymatic treatment techniques of lignin.

Supplementary Materials: The following supporting information can be downloaded at: https://www.mdpi.com/article/10.3390/en16031557/s1, Supplementary Materials and Methods: Gene cloning (Transformation), Enzyme Assays (Optimal pH, Temperature Dependence & Thermostability, Enzyme Kinetics), Enzymatic Treatment of Organosolv Lignin (Gel Permeation Chromatography, Gas Chromatography-Mass Spectrometry). Table S1: Oligonucleotide primers used for gene amplification. Figure S1: Spectra of *Sc*DyPs. Figure S2: Steady-state kinetics of *Sc*DyPs against ABTS as a substrate. Figure S3: Steady-state kinetics of *Sc*DyP2A and *Sc*DyPB against 2,6-DMP.

Author Contributions: Conceptualization, T.L. and H.P.; methodology, formal analysis and investigation, T.L., H.P., P.J. and M.I.B.; writing—original draft preparation, H.P., T.L. and P.J.; funding acquisition, T.L. All authors have read and agreed to the published version of the manuscript.

Funding: This work was supported by the European Regional Development Fund and the programme Mobilitas Pluss (grant number MOBTT60).

Data Availability Statement: All data underlying the results are available as part of the article and supplementary materials. No additional source data are required.

Acknowledgments: The authors would like to thank Priit Väljamäe for helpful discussions during the preparation of this manuscript. The contribution of COST Action LignoCOST (CA17128), supported by COST (European Cooperation in Science and Technology, www.cost.eu), in promoting interaction, exchange of knowledge and collaborations in the field of lignin valorization is gratefully acknowledged.

Conflicts of Interest: The authors declare no conflict of interest.

References

1. Dahmen, N.; Lewandowski, I.; Zibek, S.; Weidtmann, A. Integrated Lignocellulosic Value Chains in a Growing Bioeconomy: Status Quo and Perspectives. *GCB Bioenergy* **2019**, *11*, 107–117. [CrossRef]
2. Watkins, D.; Nuruddin, M.; Hosur, M.; Tcherbi-Narteh, A.; Jeelani, S. Extraction and Characterization of Lignin from Different Biomass Resources. *J. Mater. Res. Technol.* **2015**, *4*, 26–32. [CrossRef]
3. Chandel, A.K.; Garlapati, V.K.; Singh, A.K.; Antunes, F.A.F.; da Silva, S.S. The Path Forward for Lignocellulose Biorefineries: Bottlenecks, Solutions, and Perspective on Commercialization. *Bioresour. Technol.* **2018**, *264*, 370–381. [CrossRef]
4. Cao, L.; Yu, I.K.M.; Liu, Y.; Ruan, X.; Tsang, D.C.W.; Hunt, A.J. Lignin Valorization for the Production of Renewable Chemicals : State-of-the- Art Review and Future Prospects. *Bioresour. Technol.* **2018**, *269*, 465–475. [CrossRef] [PubMed]
5. Zoghlami, A.; Paës, G. Lignocellulosic Biomass: Understanding Recalcitrance and Predicting Hydrolysis. *Front. Chem.* **2019**, *7*, 874. [CrossRef] [PubMed]
6. Kumar, A.; Anushree; Kumar, J.; Bhaskar, T. Utilization of Lignin: A Sustainable and Eco-Friendly Approach. *J. Energy Inst.* **2020**, *93*, 235–271. [CrossRef]
7. Ragauskas, A.J.; Beckham, G.T.; Biddy, M.J.; Chandra, R.; Chen, F.; Davis, M.F.; Davison, B.H.; Dixon, R.A.; Gilna, P.; Keller, M.; et al. Lignin Valorization : Improving Lignin Processing in the Biorefinery. *Science* **2014**, *344*, 1246843. [CrossRef]
8. Li, C.; Zhao, X.; Wang, A.; Huber, G.W.; Zhang, T. Catalytic Transformation of Lignin for the Production of Chemicals and Fuels. *Chem. Rev.* **2015**, *115*, 11559–11624. [CrossRef]
9. Schutyser, W.; Renders, T.; Van Den Bosch, S.; Koelewijn, S.F.; Beckham, G.T.; Sels, B.F. Chemicals from Lignin: An Interplay of Lignocellulose Fractionation, Depolymerisation, and Upgrading. *Chem. Soc. Rev.* **2018**, *47*, 852–908.
10. Becker, J.; Wittmann, C. A Field of Dreams: Lignin Valorization into Chemicals, Materials, Fuels, and Health-Care Products. *Biotechnol. Adv.* **2019**, *37*, 107360.
11. Vanholme, R.; Demedts, B.; Morreel, K.; Ralph, J.; Boerjan, W. Lignin Biosynthesis and Structure. *Plant Physiol.* **2010**, *153*, 895–905. [CrossRef] [PubMed]
12. Chio, C.; Sain, M.; Qin, W. Lignin Utilization : A Review of Lignin Depolymerization from Various Aspects. *Renew. Sustain. Energy Rev.* **2019**, *107*, 232–249. [CrossRef]
13. Koranyi, T.I.; Fridrich, B.; Pineda, A.; Barta, K. Development of "Lignin-First" Approaches for the Valorization of Lignocellulosic Biomass. *Molecules* **2020**, *25*, 2815. [CrossRef] [PubMed]
14. Dessbesell, L.; Paleologou, M.; Leitch, M.; Pulkki, R.; Xu, C. Global Lignin Supply Overview and Kraft Lignin Potential as an Alternative for Petroleum-Based Polymers. *Renew. Sustain. Energy Rev.* **2020**, *123*, 109768. [CrossRef]
15. Bajwa, D.S.; Pourhashem, G.; Ullah, A.H.; Bajwa, S.G. A Concise Review of Current Lignin Production, Applications, Products and Their Environment Impact. *Ind. Crops Prod.* **2019**, *139*, 111526. [CrossRef]
16. Jõul, P.; Ho, T.T.; Kallavus, U.; Konist, A.; Leiman, K.; Salm, O.S.; Kulp, M.; Koel, M.; Lukk, T. Characterization of Organosolv Lignins and Their Application in the Preparation of Aerogels. *Materials* **2022**, *15*, 2861. [CrossRef]
17. Bauer, S.; Sorek, H.; Mitchell, V.D.; Ibáñez, A.B.; Wemmer, D.E. Characterization of Miscanthus Giganteus Lignin Isolated by Ethanol Organosolv Process under Reflux Condition. *J. Agric. Food Chem.* **2012**, *60*, 8203–8212. [CrossRef]
18. Tribot, A.; Amer, G.; Abdou Alio, M.; de Baynast, H.; Delattre, C.; Pons, A.; Mathias, J.D.; Callois, J.M.; Vial, C.; Michaud, P.; et al. Wood-Lignin: Supply, Extraction Processes and Use as Bio-Based Material. *Eur. Polym. J.* **2019**, *112*, 228–240. [CrossRef]
19. Chan, J.C.; Paice, M.; Zhang, X. Enzymatic Oxidation of Lignin: Challenges and Barriers Toward Practical Applications. *ChemCatChem* **2020**, *12*, 401–425. [CrossRef]
20. Fache, M.; Boutevin, B.; Caillol, S. Vanillin Production from Lignin and Its Use as a Renewable Chemical. *ACS Sustain. Chem. Eng.* **2016**, *4*, 35–46. [CrossRef]
21. Van Den Bosch, S.; Renders, T.; Kennis, S.; Koelewijn, S.F.; Van Den Bossche, G.; Vangeel, T.; Deneyer, A.; Depuydt, D.; Courtin, C.M.; Thevelein, J.M.; et al. Integrating Lignin Valorization and Bio-Ethanol Production: On the Role of Ni-Al_2O_3 Catalyst Pellets during Lignin-First Fractionation. *Green Chem.* **2017**, *19*, 3313–3326. [CrossRef]
22. Shuai, L.; Talebi Amiri, M.; Questell-Santiago, Y.M.; Héroguel, F.; Li, Y.; Kim, H.; Meilan, R.; Chapple, C.; Ralph, J.; Luterbacher, J.S. Formaldehyde Stabilization Facilitates Lignin Monomer Production during Biomass Depolymerization. *Science* **2016**, *354*, 329–334. [CrossRef]
23. Bugg, T.D.H.; Ahmad, M.; Hardiman, E.M.; Rahmanpour, R. Pathways for Degradation of Lignin in Bacteria and Fungi. *Nat. Prod. Rep.* **2011**, *28*, 1883–1896. [CrossRef]
24. Tian, J.; Pourcher, A.; Bouchez, T.; Gelhaye, E.; Peu, P. Occurrence of Lignin Degradation Genotypes and Phenotypes among Prokaryotes. *Appl. Microbiol. Biotechnol.* **2014**, *98*, 9527–9544. [CrossRef] [PubMed]
25. Majumdar, S.; Lukk, T.; Solbiati, J.O.; Bauer, S.; Nair, S.K.; Cronan, J.E.; Gerlt, J.A. Roles of Small Laccases from Streptomyces in Lignin Degradation. *Biochemistry* **2014**, *53*, 4047–4058. [CrossRef]
26. Janusz, G.; Pawlik, A.; Sulej, J.; Świderska-Burek, U.; Jarosz-Wilkolazka, A.; Paszczyński, A. Lignin Degradation: Microorganisms, Enzymes Involved, Genomes Analysis and Evolution. *FEMS Microbiol. Rev.* **2017**, *41*, 941–962. [CrossRef] [PubMed]
27. Li, C.; Chen, C.; Wu, X.; Tsang, C.; Mou, J.; Yan, J.; Liu, Y.; Sze, C.; Lin, K. Recent Advancement in Lignin Biorefinery: With Special Focus on Enzymatic Degradation and Valorization. *Bioresour. Technol.* **2019**, *291*, 121898. [CrossRef] [PubMed]
28. Zámocky, M.; Hofbauer, S.; Schaffner, I.; Gasselhuber, B.; Nicolussi, A.; Soudi, M.; Pirker, K.F.; Furtmüller, P.G.; Obinger, C. Independent Evolution of Four Heme Peroxidase Superfamilies. *Arch. Biochem. Biophys.* **2015**, *574*, 108–119. [CrossRef] [PubMed]

29. Kim, S.J.U.N.; Shoda, M. Purification and Characterization of a Novel Peroxidase from Geotrichum Candidum Dec 1 Involved in Decolorization of Dyes. *Appl. Environ. Microbiol.* **1999**, *65*, 1029–1035. [CrossRef]
30. Sugano, Y.; Muramatsu, R.; Ichiyanagi, A.; Sato, T.; Shoda, M. DyP, a Unique Dye-Decolorizing Peroxidase, Represents a Novel Heme Peroxidase Family: ASP171 Replaces the Distal Histidine of Classical Peroxidases. *J. Biol. Chem.* **2007**, *282*, 36652–36658. [CrossRef]
31. Kim, S.J.; Ishikawa, K.; Hirai, M.; Shoda, M. Characteristics of a Newly Isolated Fungus, Geotrichum Candidum Dec 1, Which Decolorizes Various Dyes. *J. Ferment. Bioeng.* **1995**, *79*, 601–607. [CrossRef]
32. Singh, R.; Eltis, L.D. The Multihued Palette of Dye-Decolorizing Peroxidases. *Arch. Biochem. Biophys.* **2015**, *574*, 56–65. [CrossRef] [PubMed]
33. Sugawara, K.; Nishihashi, Y.; Narioka, T.; Yoshida, T.; Morita, M.; Sugano, Y. Characterization of a Novel DyP-Type Peroxidase from Streptomyces Avermitilis. *J. Biosci. Bioeng.* **2017**, *123*, 425–430. [CrossRef]
34. Ahmad, M.; Roberts, J.N.; Hardiman, E.M.; Singh, R.; Eltis, L.D.; Bugg, T.D.H. Identification of DypB from Rhodococcus Jostii RHA1 as a Lignin Peroxidase. *Biochemistry* **2011**, *50*, 5096–5107. [CrossRef] [PubMed]
35. Liers, C.; Bobeth, C.; Pecyna, M.; Ullrich, R.; Hofrichter, M. DyP-like Peroxidases of the Jelly Fungus Auricularia Auricula-Judae Oxidize Nonphenolic Lignin Model Compounds and High-Redox Potential Dyes. *Appl. Microbiol. Biotechnol.* **2010**, *85*, 1869–1879. [CrossRef]
36. Min, K.; Gong, G.; Woo, H.M.; Kim, Y.; Um, Y. A Dye-Decolorizing Peroxidase from Bacillus Subtilis Exhibiting Substrate-Dependent Optimum Temperature for Dyes and β-Ether Lignin Dimer. *Sci. Rep.* **2015**, *5*, 8245. [CrossRef] [PubMed]
37. Fawal, N.; Li, Q.; Savelli, B.; Brette, M.; Passaia, G.; Fabre, M.; Mathé, C.; Dunand, C. PeroxiBase: A Database for Large-Scale Evolutionary Analysis of Peroxidases. *Nucleic Acids Res.* **2013**, *41*, 441–444. [CrossRef] [PubMed]
38. Yoshida, T.; Sugano, Y. A Structural and Functional Perspective of DyP-Type Peroxidase Family. *Arch. Biochem. Biophys.* **2015**, *574*, 49–55. [CrossRef]
39. Colpa, D.I.; Fraaije, M.W.; Bloois, E. Van. DyP-Type Peroxidases: A Promising and Versatile Class of Enzymes. *J. Ind. Microbiol. Biotechnol.* **2014**, *41*, 1–7. [CrossRef]
40. Salvachúa, D.; Prieto, A.; Martínez, Á.T.; Martínez, M.J. Enzyme from Irpex Lacteus and Its Application in Enzymatic Hydrolysis of Wheat Straw. *Appl. Environ. Microbiol.* **2013**, *79*, 4316–4324. [CrossRef]
41. Roberts, J.N.; Singh, R.; Grigg, J.C.; Murphy, M.E.P.; Bugg, T.D.H.; Eltis, L.D. Characterization of Dye-Decolorizing Peroxidases from Rhodococcus Jostii RHA1. *Biochemistry* **2011**, *50*, 5108–5119. [CrossRef] [PubMed]
42. Van Bloois, E.; Pazmiño, D.E.T.; Winter, R.T.; Fraaije, M.W. A Robust and Extracellular Heme-Containing Peroxidase from Thermobifida Fusca as Prototype of a Bacterial Peroxidase Superfamily. *Appl. Microbiol. Biotechnol.* **2010**, *86*, 1419–1430. [CrossRef] [PubMed]
43. Rahmanpour, R.; Bugg, T.D.H. Characterisation of Dyp-Type Peroxidases from Pseudomonas Fluorescens Pf-5: Oxidation of Mn(II) and Polymeric Lignin by Dyp1B. *Arch. Biochem. Biophys.* **2015**, *574*, 93–98. [CrossRef] [PubMed]
44. Bentley, S.D.; Chater, K.F.; Cerdeño-Tárraga, A.M.; Challis, G.L.; Thomson, N.R.; James, K.D.; Harris, D.E.; Quail, M.A.; Kieser, H.; Harper, D.; et al. Complete Genome Sequence of the Model Actinomycete Streptomyces Coelicolor A3(2). *Nature* **2002**, *417*, 141–147. [CrossRef] [PubMed]
45. Teder, T.; Lõhelaid, H.; Samel, N. Structural and Functional Insights into the Reaction Specificity of Catalase-Related Hydroperoxide Lyase: A Shift from Lyase Activity to Allene Oxide Synthase by Site-Directed Mutagenesis. *PLoS ONE* **2017**, *12*, e0185291. [CrossRef]
46. Breslmayr, E.; Hanžek, M.; Hanrahan, A.; Leitner, C.; Kittl, R.; Šantek, B.; Oostenbrink, C.; Ludwig, R. A Fast and Sensitive Activity Assay for Lytic Polysaccharide Monooxygenase. *Biotechnol. Biofuels* **2018**, *11*, 79. [CrossRef]
47. Ollinger, J.; Song, K.B.; Antelmann, H.; Hecker, M.; Helmann, J.D. Role of the Fur Regulon in Iron Transport in Bacillus Subtilis. *J. Bacteriol.* **2006**, *188*, 3664–3673. [CrossRef] [PubMed]
48. Biswas, L.; Biswas, R.; Nerz, C.; Ohlsen, K.; Schlag, M.; Schäfer, T.; Lamkemeyer, T.; Ziebandt, A.K.; Hantke, K.; Rosenstein, R.; et al. Role of the Twin-Arginine Translocation Pathway in Staphylococcus. *J. Bacteriol.* **2009**, *191*, 5921–5929. [CrossRef]
49. Létoffé, S.; Heuck, G.; Delepelaire, P.; Lange, N.; Wandersman, C. Bacteria Capture Iron from Heme by Keeping Tetrapyrrol Skeleton Intact. *Proc. Natl. Acad. Sci. USA* **2009**, *106*, 11719–11724. [CrossRef]
50. Zitare, U.A.; Habib, M.H.; Rozeboom, H.; Mascotti, M.L.; Todorovic, S.; Fraaije, M.W. Mutational and Structural Analysis of an Ancestral Fungal Dye-Decolorizing Peroxidase. *FEBS J.* **2021**, *288*, 3602–3618. [CrossRef]
51. Jeong, H.; Barbe, V.; Lee, C.H.; Vallenet, D.; Yu, D.S.; Choi, S.H.; Couloux, A.; Lee, S.W.; Yoon, S.H.; Cattolico, L.; et al. Genome Sequences of Escherichia Coli B Strains REL606 and BL21(DE3). *J. Mol. Biol.* **2009**, *394*, 644–652. [CrossRef] [PubMed]
52. Rosano, G.L.; Ceccarelli, E.A. Recombinant Protein Expression in Escherichia Coli: Advances and Challenges. *Front. Microbiol.* **2014**, *5*, 172. [CrossRef] [PubMed]
53. Rosano, G.L.; Morales, E.S.; Ceccarelli, E.A. New Tools for Recombinant Protein Production in Escherichia Coli: A 5-Year Update. *Protein Sci.* **2019**, *28*, 1412–1422. [CrossRef] [PubMed]
54. Lithwick, G.; Margalit, H. Hierarchy of Sequence-Dependent Features Associated with Prokaryotic Translation. *Genome Res.* **2003**, *13*, 2665–2673. [CrossRef] [PubMed]
55. Gustafsson, C.; Govindarajan, S.; Minshull, J. Codon Bias and Heterologous Protein Expression. *Trends Biotechnol.* **2004**, *22*, 346–353. [CrossRef]

56. Al-Hawash, A.B.; Zhang, X.; Ma, F. Strategies of Codon Optimization for High-Level Heterologous Protein Expression in Microbial Expression Systems. *Gene Rep.* **2017**, *9*, 46–53. [CrossRef]
57. Johansson, A.S.; Bolton-Grob, R.; Mannervik, B. Use of Silent Mutations in CDNA Encoding Human Glutathione Transferase M2-2 for Optimized Expression in Escherichia Coli. *Protein Expr. Purif.* **1999**, *17*, 105–112. [CrossRef]
58. Jung, Y.; Kwak, J.; Lee, Y. High-Level Production of Heme-Containing Holoproteins in Escherichia Coli. *Appl. Microbiol. Biotechnol.* **2001**, *55*, 187–191. [CrossRef]
59. Chouchane, S.; Lippai, I.; Magliozzo, R.S. Catalase-Peroxidase (Mycobacterium Tuberculosis KatG) Catalysis and Isoniazid Activation. *Biochemistry* **2000**, *39*, 9975–9983. [CrossRef]
60. Sudhamsu, J.; Kabir, M.; Airola, M.V.; Patel, B.A.; Yeh, S.R.; Rousseau, D.L.; Crane, B.R. Co-Expression of Ferrochelatase Allows for Complete Heme Incorporation into Recombinant Proteins Produced in E. Coli. *Protein Expr. Purif.* **2010**, *73*, 78–82. [CrossRef]
61. Varnado, C.L.; Goodwin, D.C. System for the Expression of Recombinant Hemoproteins in Escherichia Coli. *Protein Expr. Purif.* **2004**, *35*, 76–83. [CrossRef] [PubMed]
62. Sugano, Y.; Nakano, R.; Sasaki, K.; Shoda, M. Efficient Heterologous Expression in Aspergillus Oryzae of a Unique Dye-Decolorizing Peroxidase, DyP, of Geotrichum Candidum Dec 1. *Appl. Environ. Microbiol.* **2000**, *66*, 1754–1758. [CrossRef] [PubMed]
63. Sugawara, K.; Yoshida, T.; Hirashima, R.; Toriumi, R.; Akiyama, H.; Kakuta, Y.; Ishige, Y.; Sugano, Y. Characterization of Class V DyP-Type Peroxidase SaDyP1 from Streptomyces Avermitilis and Evaluation of SaDyPs Expression in Mycelium. *Int. J. Mol. Sci.* **2021**, *22*, 8683. [CrossRef] [PubMed]
64. Linde, D.; Ayuso-Fernández, I.; Laloux, M.; Aguiar-Cervera, J.E.; de Lacey, A.L.; Ruiz-Dueñas, F.J.; Martínez, A.T. Comparing Ligninolytic Capabilities of Bacterial and Fungal Dye-Decolorizing Peroxidases and Class-Ii Peroxidase-Catalases. *Int. J. Mol. Sci.* **2021**, *22*, 2629. [CrossRef]
65. Rodrigues, C.F.; Borges, P.T.; Scocozza, M.F.; Silva, D.; Taborda, A.; Brissos, V.; Frazão, C.; Martins, L.O. Loops around the Heme Pocket Have a Critical Role in the Function and Stability of Bsdyp from Bacillus Subtilis. *Int. J. Mol. Sci.* **2021**, *22*, 10862. [CrossRef]
66. Chaplin, A.K.; Wilson, M.T.; Worrall, J.A.R. Kinetic Characterisation of a Dye Decolourising Peroxidase from Streptomyces Lividans: New Insight into the Mechanism of Anthraquinone Dye Decolourisation. *Dalt. Trans.* **2017**, *46*, 9420–9429. [CrossRef]
67. Liu, Y.; Huang, L.; Guo, W.; Jia, L.; Fu, Y.; Gui, S.; Lu, F. Cloning, Expression, and Characterization of a Thermostable and PH-Stable Laccase from Klebsiella Pneumoniae and Its Application to Dye Decolorization. *Process Biochem.* **2017**, *53*, 125–134. [CrossRef]
68. Arregui, L.; Ayala, M.; Gómez-Gil, X.; Gutiérrez-Soto, G.; Hernández-Luna, C.E.; Herrera De Los Santos, M.; Levin, L.; Rojo-Domínguez, A.; Romero-Martínez, D.; Saparrat, M.C.N.; et al. Laccases: Structure, Function, and Potential Application in Water Bioremediation. *Microb. Cell Fact.* **2019**, *18*, 200. [CrossRef]
69. Chen, C.; Shrestha, R.; Jia, K.; Gao, P.F.; Geisbrecht, B.V.; Bossmann, S.H.; Shi, J.; Li, P. Characterization of Dye-Decolorizing Peroxidase (DyP) from Thermomonospora Curvata Reveals Unique Catalytic Properties of A-Type DyPs. *J. Biol. Chem.* **2015**, *290*, 23447–23463. [CrossRef]
70. Kokkonen, P.; Beier, A.; Mazurenko, S.; Damborsky, J.; Bednar, D.; Prokop, Z. Substrate Inhibition by the Blockage of Product Release and Its Control by Tunnel Engineering. *RSC Chem. Biol.* **2021**, *2*, 645–655. [CrossRef]
71. Benslama, O.; Mansouri, N.; Arhab, R. In Silico Investigation of the Lignin Polymer Biodegradation by Two Actinomycetal Peroxidase Enzymes. *Mater. Today Proc.* **2022**, *53*, 1–5. [CrossRef]
72. Gilbert, R.G.; Hess, M.; Jenkins, A.D.; Jones, R.G.; Kratochvíl, P.; Stepto, R.F.T. Dispersity in Polymer Science (IUPAC Recommendations 2009). *Pure Appl. Chem.* **2009**, *81*, 351–353.
73. Kim, K.H.; Kim, C.S. Recent Efforts to Prevent Undesirable Reactions from Fractionation to Depolymerization of Lignin: Toward Maximizing the Value from Lignin. *Front. Energy Res.* **2018**, *6*, 92. [CrossRef]
74. Vignali, E.; Gigli, M.; Cailotto, S.; Pollegioni, L.; Rosini, E.; Crestini, C. The Laccase-Lig Multienzymatic Multistep System in Lignin Valorization. *ChemSusChem* **2022**, *15*, e202201147. [CrossRef]
75. Rahmanpour, R.; King, L.D.W.; Bugg, T.D.H. Identification of an Extracellular Bacterial Flavoenzyme That Can Prevent Re-Polymerisation of Lignin Fragments. *Biochem. Biophys. Res. Commun.* **2017**, *482*, 57–61. [CrossRef]
76. Musengi, A.; Durrell, K.; Prins, A.; Khan, N.; Agunbiade, M.; Kudanga, T.; Kirby-McCullough, B.; Pletschke, B.I.; Burton, S.G.; Le Roes-Hill, M. Production and Characterisation of a Novel Actinobacterial DyP-Type Peroxidase and Its Application in Coupling of Phenolic Monomers. *Enzyme Microb. Technol.* **2020**, *141*, 109654. [CrossRef]

Disclaimer/Publisher's Note: The statements, opinions and data contained in all publications are solely those of the individual author(s) and contributor(s) and not of MDPI and/or the editor(s). MDPI and/or the editor(s) disclaim responsibility for any injury to people or property resulting from any ideas, methods, instructions or products referred to in the content.